Journal of Alloys and Compounds 507 (2010) 162–166

Contents lists available at ScienceDirect

Journal of Alloys and Compounds

journal homepage: www.elsevier.com/locate/jallcom

Texture and magnetostriction studies in Bridgman solidified $Ho_{0.85}Tb_{0.15}Fe_{1.95}$ alloys

J. Arout Chelvane*, S. Banumathy, Mithun Palit, Himalay Basumatary, A.K. Singh, S. Pandian

Defence Metallurgical Research Laboratory, Kanchanbagh, Hyderabad 500058, India

ARTICLE INFO

Article history:
Received 11 June 2010
Received in revised form 19 July 2010
Accepted 21 July 2010
Available online 29 July 2010

Keywords:
Magnetostriction
Laves phase
Grain orientation

ABSTRACT

This work describes the evolution of texture in anisotropy compensated $Ho_{0.85}Tb_{0.15}Fe_{1.95}$ alloy which was conventionally cast and directionally solidified at four different growth rates by adopting modified Bridgman technique. The development of texture as a function of solidification rate has been investigated by analyzing the experimental X-ray pole figures. A strong ⟨3 1 1⟩ texture component has been observed for the sample solidified at lower growth rate and mixed texture components of ⟨3 1 1⟩, ⟨112⟩, ⟨3 3 1⟩ ⟨5 3 1⟩ and ⟨1 1 0⟩ for the samples solidified at higher growth rate. Consequently, larger magnetostriction has been observed in the sample solidified at lower growth rate than in those solidified at higher growth rate.

© 2010 Elsevier B.V. All rights reserved.

1. Introduction

The research and development on the giant magnetostrictive materials (RFe_2: R-rare earth) is being pursued with profound interest for several years due to its wider implication in revolutionizing magnetostrictive actuators and transducers [1–3]. A large initial magnetostriction (or large $d\lambda/dH$) is considered as the figure of merit while designing a transducer or an actuator. This condition is generally met by growing the material in cylindrical rod form with preferred grain orientation and by controlling the alloy chemistry to yield a microstructure consisting of only the giant magnetostrictive phase. Directional solidification by float zone technique (for rods of smaller diameter ~10 mm or less) and modified Bridgman (MB) technique (for rods of larger diameter >10 mm) are commonly adopted to impart the desired grain orientation in these materials [3]. The processing conditions such as solidification rate (v) and temperature gradient (G), affect the resultant texture of the directionally solidified rod. Among several rare earth–iron intermetallics, the cubic Laves phase (C15 type) RFe_2 compounds display giant magnetostriction and large magnetocrystalline anisotropy. In an effort to decrease the magnetocrystalline anisotropy and thereby reduce the level of bias field requirement, anisotropy compensated mixed rare earth alloys such as $(Tb,Dy)Fe_2$, $(Ho,Tb)Fe_2$ and $(Tb,Pr)Fe_2$ etc. have been evolved [1]. Among these, the $(Tb,Dy)Fe_2$ exhibiting large magnetostriction has been extensively studied both from fundamental and technological perspectives, while $(Tb,Pr)Fe_2$ to a lesser extent owing to the existence of additional phases such as $(Tb,Pr)Fe_3$, (Tb,Pr)-rich, $(Tb,Pr)_2Fe_{17}$ which appear even for smaller substitution of Pr for Tb. Both $(Tb,Dy)Fe_2$ and $(Tb,Pr)Fe_2$ phases are formed as a result of incomplete peritectic reaction [L (liquid) + $RFe_3 \rightarrow RFe_2$] and as a result some remanent pro-peritectic RFe_3 phase detrimental to magnetostriction is seen in the microstructure [1,4,5]. In contrast to these two anisotropy compensated pseudo-binary systems *viz.*, (Tb,Dy)-Fe and (Tb,Pr)-Fe mentioned above, the Ho–Tb–Fe system has an advantage since the gap between liquidus and $(Ho,Tb)Fe_2$ peritectic temperature is almost negligible. Hence by adopting directional solidification with high temperature gradient the formation of detrimental pro-peritectic $(Ho,Tb)Fe_3$ phase can be suppressed. Although there are several reports on the magnetic properties of this system, the effect of grain orientation and its relation to magnetostriction is still elusive [6,7]. In this context, a study was carried out to directionally solidify $Ho_{0.85}Tb_{0.15}Fe_{1.95}$ alloy at different growth rates by modified Bridgman technique and investigate the texture development. An attempt has also been made to bring out correlations between texture and magnetostriction in this material.

2. Experimental details

Alloy of nominal composition, $Ho_{0.85}Tb_{0.15}Fe_{1.95}$, was prepared by melting the high pure elemental ingredients in a vacuum induction furnace and casting the liquid alloy in quartz tubes of 20 mm diameter placed over water cooled copper plate. The cast rod was then directionally solidified by adopting modified Bridgman technique under vacuum (~10^{-5} mbar). Directional solidification experiments were carried out by placing the chill cast rod on retractable water-cooled copper chill plate, which was then lowered from hot zone (1350 °C) at various solidification rates. The initial temperature gradient that could be achieved was 100 °C/cm. Directionally solidified samples were obtained for four different pulling rates *viz.* 7, 35, 70 and 100 cm/h.

* Corresponding author. Tel.: +91 40 24586677; fax: +91 40 24340884.
E-mail address: jarout@yahoo.com (J.A. Chelvane).

0925-8388/$ – see front matter © 2010 Elsevier B.V. All rights reserved.
doi:10.1016/j.jallcom.2010.07.145

The directionally solidified rods were then annealed at 950 °C/4 days under high vacuum (~10^{-5} mbar). Using a Leo 440i scanning electron microscope (SEM) the microstructure of the annealed samples was investigated and identification of the different phases present in the samples was done with the aid of micro-chemical analysis and X-ray micrographs. The evolution of texture during directional solidification at different rates was characterized by obtaining incomplete experimental pole figures by rotating the test sample cut perpendicular to the axis of the rod around normal direction (ϕ) and transverse direction (χ). A continuous translation (±8 mm) has been employed to scan large sample area. The Inel XRG 3000 diffractometer coupled with curved 'position sensitive detector' and Cu Kα radiation has been used for this purpose. The obtained pole figures were analyzed using Labotex software to obtain the angular co-ordinates (χ, ϕ) of high intensity contours. The observed angular co-ordinates were compared with standard stereograms of C15 Laves phase to determine the texture components. The room temperature static magnetostriction was measured under dc magnetic field using field compensated resistance strain gauges.

3. Results and discussions

The conventionally cast and annealed directionally solidified [7,35, 70 and 100 cm/h] $Ho_{0.85}Tb_{0.15}Fe_{1.95}$ samples exhibit a near uniform chemical composition along the entire length of the rod with the microstructure of it displaying (Ho,Tb)Fe_2 phase as the major phase and (Ho,Tb)-rich phase as minor phase [Fig. 1].

3.1. Texture studies

The X-ray pole figures of the directionally solidified $Ho_{0.85}Tb_{0.15}Fe_{1.95}$ rods corresponding to the different pulling rates *viz.*, 7, 35, 70 and 100 cm/h are shown in Fig. 2a–d respectively. The description of the texture components, as observed from (2 2 0), (3 1 1) and (4 2 2) pole figures, are presented briefly as a function of pulling rates.

Sample solidified at 7 cm/h: The (3 1 1) pole figure of the sample exhibits high intensity at $\chi = 1°$, indicating a strong ⟨3 1 1⟩ texture component. The presence of strong ⟨3 1 1⟩ texture component is further seen at $\chi = 64°$ of (2 2 0) pole figure and at $\chi = 10.7°$ of (4 2 2) pole figure. Thus, the sample solidified at 7 cm/h exhibits only ⟨3 1 1⟩ as the major texture component [8].

Sample solidified at 35 cm/h: The (2 2 0) pole figure of the sample exhibits high intensity at $\chi = 55°$, from which the presence of ⟨1 1 2⟩ texture component is inferred. Along with ⟨1 1 2⟩ texture component, ⟨3 1 1⟩ texture component is also present at $\chi = 35.3°$ of (3 1 1) pole figure. Interestingly, a third component ⟨5 3 1⟩ is also observed at a location $\chi = 45°$ of the (4 2 2) pole figure.

Sample solidified at 70 cm/h: The sample solidified at 70 cm/h show three major texture components *viz.*, ⟨3 1 1⟩, ⟨3 3 1⟩ and ⟨1 1 2⟩ of nearly equal intensities. The presence of ⟨3 1 1⟩ texture component, located at the centre of the pole figure, is seen at $\chi = 3°$ of (3 1 1) pole figure. It is observed from the same pole figure that, in addition to ⟨3 1 1⟩ orientation, ⟨1 1 2⟩ texture component ($\chi = 44.7°$) is also present. The high intensity at $\chi = 4.2°$ of (4 2 2) pole figure and $\chi = 55.1°$ of (2 2 0) pole figure further confirms the presence of ⟨1 1 2⟩ texture component. Apart from these texture components, a strong ⟨1 3 3⟩ texture component is also present as inferred from the intensity contour at $\chi = 71.6°$ and $\chi = 11.5°$ of (2 2 0) pole figure.

Sample solidified at 100 cm/h: The (3 1 1) pole figure of the sample exhibits the presence of ⟨5 3 1⟩ texture component located at $\chi = 45°$ and 30.3° and ⟨1 1 0⟩ texture component located at $\chi = 65.1°$. The presence of ⟨1 1 0⟩ texture component is further reconfirmed from the intensity located at $\chi = 27.3°$ of (4 2 2) pole figure. These two texture components are accompanied by ⟨1 3 3⟩ texture component with high intensity at $\chi = 16.6°$ of (2 2 0) pole figure.

The formation of ⟨3 1 1⟩ texture component at lower growth rate (7 cm/h) is attributed to higher atomic packing density (85%) of (3 1 1) plane as compared to 82% and 71% atomic packing density of (1 1 0) and (1 1 2) planes respectively. Therefore, the (3 1 1) plane forms low energy interface with liquid resulting in the growth of ⟨3 1 1⟩ as favored texture component at lower growth rate. However, the kinetics of atomic attachment to (3 1 1) plane is sluggish due to less accommodation factor. Hence, at higher growth rate ⟨1 1 0⟩, ⟨1 1 2⟩ components evolves as preferred growth orientations, owing to faster attachment of atoms to (1 1 0) and (1 1 2)

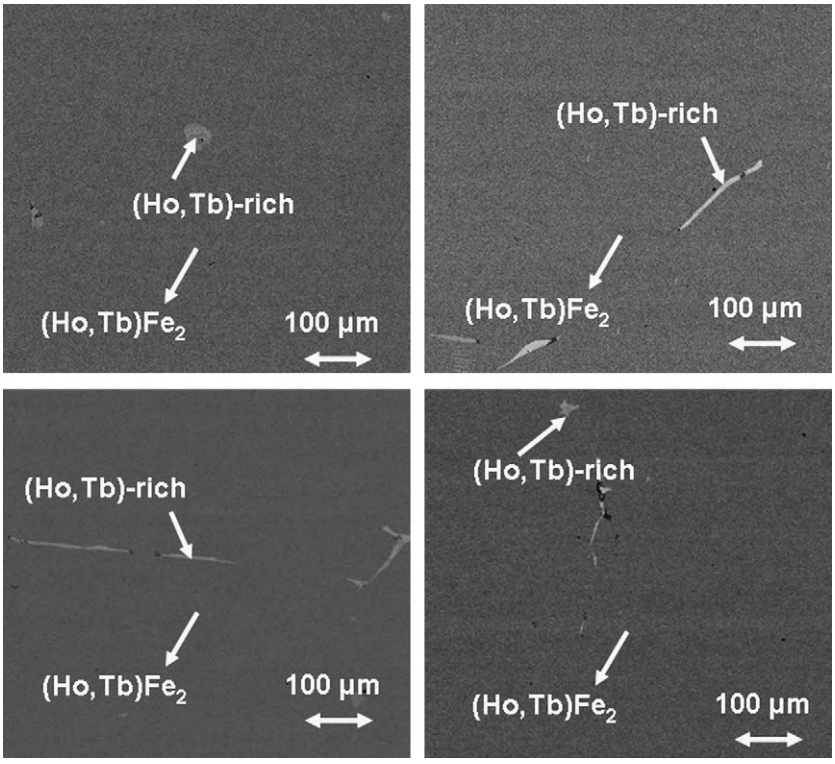

Fig. 1. Back scattered electron image of directionally solidified $Ho_{0.85}Tb_{0.15}Fe_{1.95}$ sample grown at 7, 35, 70 and 100 cm/h.

planes, which are having lesser packing density. Although, (1 1 1) plane possesses highest atomic packing density (95%), the growth of ⟨1 1 1⟩ orientation has not been noticed even with the slowest growth rate (7 cm/h) adopted in this study. This is attributed to the very sluggish attachment of atoms at the solid liquid interface due to least atomic accommodation factor of (1 1 1) plane. At higher growth rate, the evolving components such as ⟨1 1 0⟩ and ⟨1 1 2⟩ also undergo tilt during solidification and accordingly ⟨3 3 1⟩ and ⟨5 3 1⟩ components were also observed. These components can be called as 'rotated ⟨1 1 0⟩' and 'rotated ⟨1 1 2⟩>' respectively.

A summary of major texture components observed in the Bridgman solidified samples grown at different rates are presented in Table 1.

Table 1
Summary of texture components observed for samples solidified at different growth rates.

Growth rate	Major texture components
7 cm/h	⟨3 1 1⟩ and ⟨1 1 0⟩
35 cm/h	⟨3 1 1⟩, ⟨5 3 1⟩ (rotated ⟨1 1 2⟩[a]) and ⟨1 1 2⟩
70 cm/h	⟨3 1 1⟩, ⟨3 3 1⟩ (rotated ⟨1 1 0⟩[b]) and ⟨1 1 2⟩
100 cm/h	⟨5 3 1⟩, ⟨3 3 1⟩ and ⟨1 1 0⟩

[a] ⟨5 3 1⟩ (rotated ⟨1 1 2⟩) → ⟨5 3 1⟩ ~14° away from ⟨1 1 2⟩.
[b] ⟨3 3 1⟩ (rotated ⟨1 1 0⟩) → ⟨3 3 1⟩ ~13° away from ⟨1 1 0⟩.

3.2. Magnetostriction

The variation of magnetostriction as a function of applied dc magnetic field for cast and directionally solidified $Ho_{0.85}Tb_{0.15}Fe_{1.95}$ samples is shown in Fig. 3. The improvement in magnetostriction brought about by directional solidification is remarkably high compared to that obtained in the cast alloy. It is also seen that lower solidification rate (7 cm/h) is beneficial to realize large magnetostriction coupled with a sharp rise in the initial magnetostriction. This is attributed to the strong ⟨3 1 1⟩ texture which is present as single component inducing a strong magneto-elastic coupling along the entire sample. With increase in solidification rate, the magnetostriction decreases due to the presence of multiple texture components such as ⟨5 3 1⟩, ⟨3 3 1⟩, ⟨1 1 0⟩ and ⟨1 1 2⟩ in addition to ⟨3 1 1⟩ texture component. Due to the presence of multiple components the magneto-elastic coupling is found to be affected, as

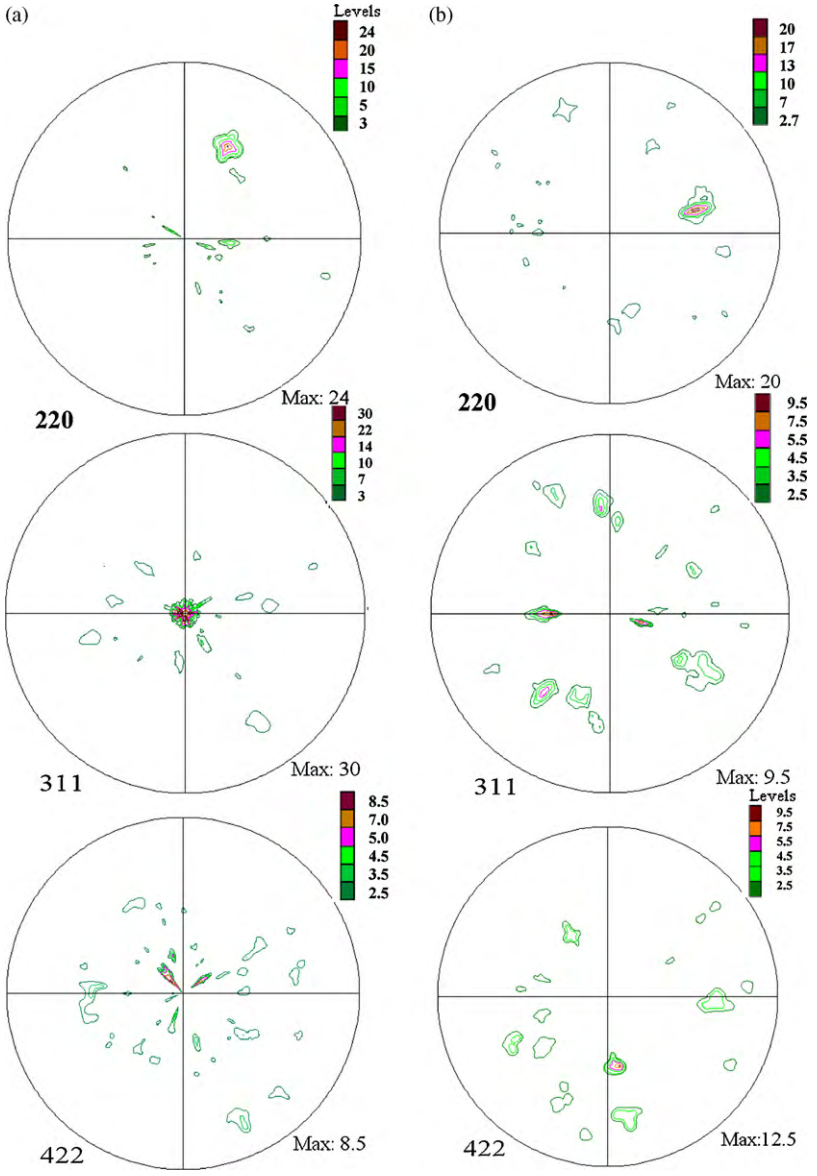

Fig. 2. (2 2 0), (3 1 1) and (4 2 2) pole figures taken on transverse section of the sample solidified at (a) 7 cm/h, (b) 35 cm/h, (c) 70 cm/h and (d) 100 cm/h.

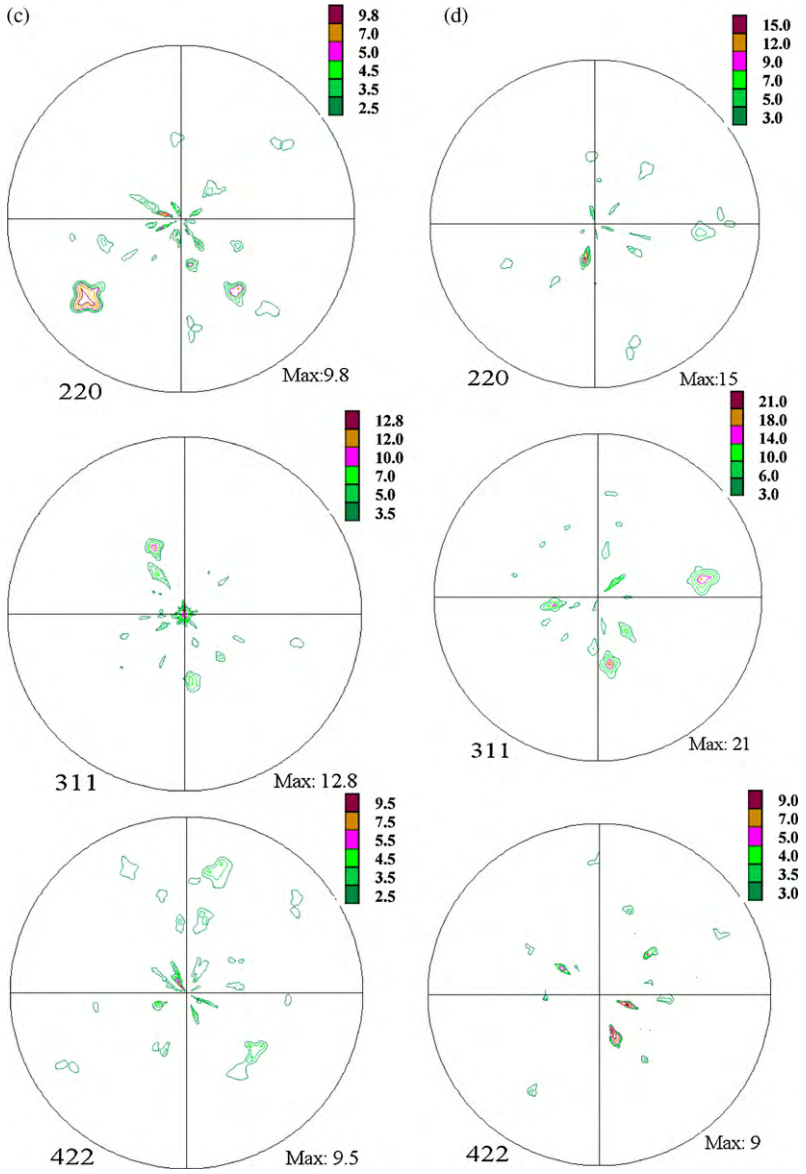

Fig. 2. (*Continued*)

each texture component having different angular relationship with the easy magnetization direction leading to incoherent domain motions under applied field. Therefore, magnetostriction is found to decrease in the sample solidified at higher growth rates.

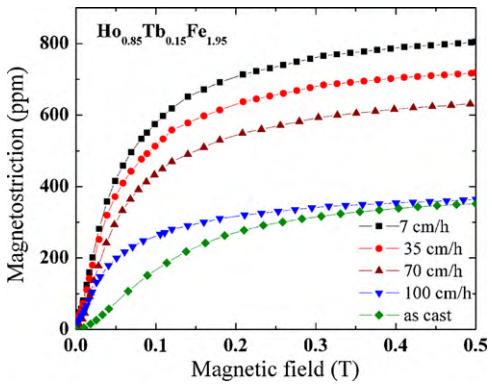

Fig. 3. Variation of magnetostriction as a function of applied magnetic field for as cast and directionally solidified (7, 35, 70 and 100 cm/h) samples.

4. Summary and conclusions

The evolution of texture with solidification rate has been correlated with magnetostriction. Low solidification rates favor large magnetostriction owing to the strong single ⟨3 1 1⟩ texture component along the growth direction. Increase in solidification rate decreases magnetostriction due to the presence of mixed grain orientations leading to poor magneto-elastic coupling.

Acknowledgements

The authors wish to thank the Defence Research and Development Organization for financial support and the Director, Defence Metallurgical Research Laboratory, for his encouragement and permission to publish this work.

References

[1] A.E. Clark, in: E.P. Wohlfarth (Ed.), Ferromagnetic Materials, North-Holland, Amsterdam, 1980, p. 531.
[2] S.W. Meeks, R.W. Timme, J. Acoust. Soc. Am. 62 (1977) 1158.

[3] Mithun Palit, S. Pandian, R. Balamuralikrishnan, A.K. Singh, Niranjan Das, V. Chandrasekharan, G. Markandeyulu, J. Appl. Phys. 100 (2006), 074913–1.
[4] Mithun Palit, J. Arout Chelvane, S. Pandian, M. Manivel Raja, V. Chandrasekaran, Mater. Char. 60 (2009) 40.
[5] J. Arout Chelvane, Mithun Palit, Himalay Basumatary, S. Pandian, V. Chandrasekaran, Phys. B 404 (2009) 1432.
[6] U. Atzmony, M.P. Dariel, E.R. Bauminger, D. Lebenbaum, I. Nowik, S. Ofer, Phys. Rev. Lett. 28 (1972) 224.
[7] K.R. Dhilsha, K.V.S. Rama Rao, J. Appl. Phys. 68 (1990) 259.
[8] B.D. Cullity, Elements of X-Ray Diffraction, Addison-Wesley Publishing Company, Reading, MA, 1978.